Renewable Energy 58 (2013) 115–126

Contents lists available at SciVerse ScienceDirect

Renewable Energy

journal homepage: www.elsevier.com/locate/renene

Extracting fatigue damage parts from the stress–time history of horizontal axis wind turbine blades

Panu Pratumnopharat [a,*], Pak Sing Leung [b], Richard S. Court [c]

[a] Mechanical Engineering Department, Faculty of Engineering, Rajamangala University of Technology Thanyaburi, Klong 6, Thanyaburi, Pathumtani 12110, Thailand
[b] Mechanical Engineering Division, School of Computing, Engineering and Information Sciences, Northumbria University, Ellison Place, Newcastle upon Tyne NE1 8ST, UK
[c] National Renewable Energy Centre, NaREC, Eddie Ferguson House, Ridley Street, Blyth NE24 3AG, UK

ARTICLE INFO

Article history:
Received 2 September 2012
Accepted 4 March 2013
Available online 9 April 2013

Keywords:
Short-time Fourier transform
Spectral density function
Load history
Load history reconstruction
Variable amplitude fatigue

ABSTRACT

Horizontal axis wind turbine (HAWT) blades are a critical component of wind turbines. Full-scale blade fatigue testing is required to verify that the blades possess the strength and service life specified in the design. Unfortunately, fatigue tests must be run for a long time period, which has led blade testing laboratories to seek ways of accelerating fatigue testing time and reducing the costs of tests. The objective of this article is to propose a concept of applying accumulative power spectral density (AccPSD) to identify fatigue damage events contained in the stress–time history of HAWT blades. Based on short-time Fourier transform (STFT), a novel method called STFT-based fatigue damage part extracting method has been developed to extract fatigue damage parts from the stress–time history and to generate the edited stress–time history. It has been found that a STFT window size of 256 and an AccPSD level of 9800 Energy/Hz (cutoff level) provides the edited stress–time history having reduction of 15.38% in length with respect to the original length, whilst fatigue damage per repetition can be retained almost the same level as the original fatigue damage. In addition, an existing method, time correlated fatigue damage (TCFD), is used to validate the effectiveness of STFT-based fatigue damage part extracting method. The results suggest that not only does the STFT improve the accuracy of fatigue damage retained, but also it provides a shorter length of the edited stress–time history. To conclude, STFT is suggested as an alternative technique in fatigue durability study, especially for the field of wind turbine engineering.

1. Introduction

Modern wind turbines are fatigue critical machines [1] used to generate electricity from the wind. These rotating machines are subject to a combination of several loadings that are highly irregular in nature. Generally, wind turbine blades are considered as an important part of the wind turbine [2]. The problem of interest is that the wind turbine blades have failed at unexpectedly high rates. The major cause of the failure is fatigue due to cyclic loading [3]. Fatigue is an engineering terminology defined as the process of initiation and propagation of cracks through a structural part due to action of fluctuating stress [4].

The unexpectedly high rate of the blade failure led designers and researchers to develop fatigue analysis capabilities to prevent blade breakage. After finalising the aerodynamic design of any new blade, full-scale blade fatigue testing is required to verify that the blades possess the strength and service life specified in the design. Fatigue lifetime of the blades of over 20 years is one of the structural design requirements specified by the IEC 61400-1 standard [5]. Laboratory based accelerated testing needs to expose the component to an equivalent test loading which is shorter in time than the length of the target loading, whilst still causing approximately the same damage potential. Techniques that can be used to accelerate laboratory fatigue testing [6] are to increase the frequency of the cyclic loading, to increase the load level and to remove small amplitude cycles from the time history. Testing time and cost can become too expensive if the service load is not edited before testing.

At present, it is found in the wind turbine community that the racetrack method [7,8] is the only existing method used in editing fatigue loading. The racetrack method is used to produce a condensed history in which essential peaks and valleys are listed in their original sequence. By removing small amplitude cycles from

* Corresponding author. Tel.: +66 (0) 2 549 3430.
E-mail addresses: panu.pratumnopharat@yahoo.com, panu.pratumnopharat@rmutt.ac.th (P. Pratumnopharat).

0960-1481/$ – see front matter © 2013 Elsevier Ltd. All rights reserved.
http://dx.doi.org/10.1016/j.renene.2013.03.009

Nomenclature

f	frequency
$G(f_n)$	power spectrum
N	number of cycles to failure
S	maximum applied stress
$S(f_n)$	power spectral density
T	period
t	time
w	window function
x	amplitude of time-domain signal
Δf	frequency band
Δt	time window length
σ	maximum applied stress
σ_0	ultimate strength
τ	time position of the window
AccPSD	accumulative power spectral density
BEMT	blade element momentum theory
FFT	fast Fourier transform
HAWT	horizontal axis wind turbine
nfft	window size
PSD	power spectral density
rms	root-mean-square
SERI	Solar Energy Research Institute
STFT	short-time Fourier transform
TCFD	time correlated fatigue damage

the time history, this method is useful for condensing histories to those few events, perhaps the 10 percent of events that do most of the damage [9–11]. Unfortunately, the racetrack method does not significantly shorten the length of the fatigue loading, and does not serve the purpose of reducing the testing time.

This is the problem that motivated the authors' interest in fatigue data editing by removing small amplitude cycles. Such a method is defined as a method for omitting the small amplitude cycles which provide a minimal contribution to the overall fatigue damage, whilst retaining the high amplitude cycles which are the most damaging sections [6]. In wind turbine applications, this concept is still not proposed for the purpose of achieving accelerated fatigue tests which reduce testing time and energy cost. Furthermore, review of the literature suggests that there is no fatigue data editing technique that used STFT for identifying and extracting fatigue damage parts from the stress–time history of horizontal axis wind turbine (HAWT) blades.

2. Material and methods

The HAWT blade used in this study is a SERI-8 blade model as shown in Fig. 1 [12]. The SERI-8 blades are installed on 65 kW wind turbines. The fibreglass composite material used in modelling the blade is a laminate called DD16 [13]. The S–N model of material DD16 is described by three-parameter model.

$$\sigma_0 - \sigma = a\sigma(\sigma/\sigma_0)^b(N^c - 1) \tag{1}$$

where σ is the maximum applied stress, σ_0 is the ultimate strength (625 MPa for tensile or 400 MPa for compressive), N is the number of cycles to failure, and a, b, c are fitting parameters which can be found in Ref. [14].

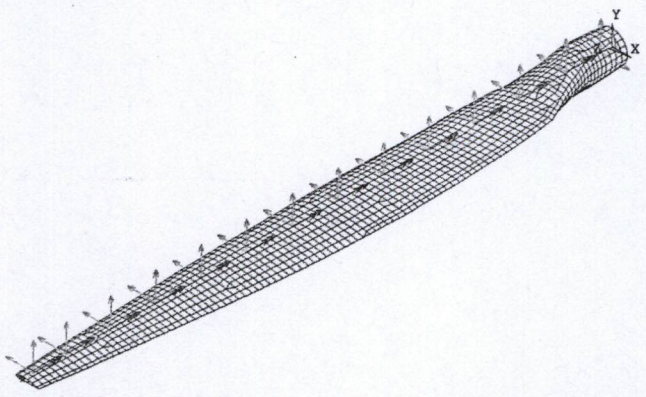

Fig. 1. Finite element model of the wind turbine blade and a set of aerodynamic loads.

A set of aerodynamic loads typically shown in Fig. 1 is generated by an aerodynamic code [15] based on blade element momentum (BEM) theory. In this study, there are number of aerodynamic load sets for wind speeds ranging from cut-in to cut-out. Each set of aerodynamic loads and finite element model are imported to ANSYS to determine a critical stress and its location on the blade. By relating the critical stress at each wind speed to the wind speed data [16], a fatigue computer code for HAWT blades [17] is used to generate a stress–time history as shown in Fig. 12(a). This history has sampling rate of 40 Hz for 68,739,939 data points which gave the total record length of the signal of 1,718,498.475 s. In this article, this history will be edited by an existing method called time correlated fatigue damage (TCFD) [18] and STFT. Then, the fatigue damage is evaluated by Miner's rule [19].

2.1. Accumulative power spectral density

In this article, STFT is used to generate a plot of accumulative power spectral density (AccPSD) as shown in Fig. 2(d). The plot of AccPSD used in the process of extracting fatigue damage parts is discussed in Section 2.2. For illustration purpose, the authors use Fig. 2 to describe how to generate the plot of AccPSD. By using signal processing toolbox in Matlab [20], STFT (with nfft = 4, noverlap = 3, fs = 40 Hz) is taken to the typical stress–time history in Fig. 2(a). Matlab generates the spectrogram shown in Fig. 2(b). Changing plotting style from spectrogram to the 3D-stem plot shown in Fig. 2(c) illustrates the relationship between PSD and frequency at each time interval (or data point number). Thus, AccPSD at each time interval is easily derived by summing the PSD of each frequency band at each time interval. For example, AccPSD at data point number 2 is the summation of three PSDs located at frequency bands 0, 10 and 20 Hz, and so on. In this manner, the plot of AccPSD distribution can be generated as shown in Fig. 2(d).

2.2. Algorithm for extracting fatigue damage parts

This section deals with how to extract fatigue damage parts from the stress–time history. The authors' use Fig. 3 to demonstrate how to extract fatigue damage parts and how to generate the edited stress–time history. Considering Fig. 3, the typical stress–time history consists of 20 data points. It is divided into 17 windows with their widths given by 4 data points. AccPSD of the signal segment in each window is represented by the spike labelled by the italic number. Since each value of AccPSD is the value at the middle of each window, there is no middle data point to locate each AccPSD spike because the number of data points in each window is even. In this case, Matlab locates each AccPSD spike at the left point nearest the middle. For example, window 1 consists of data points 1, 2, 3

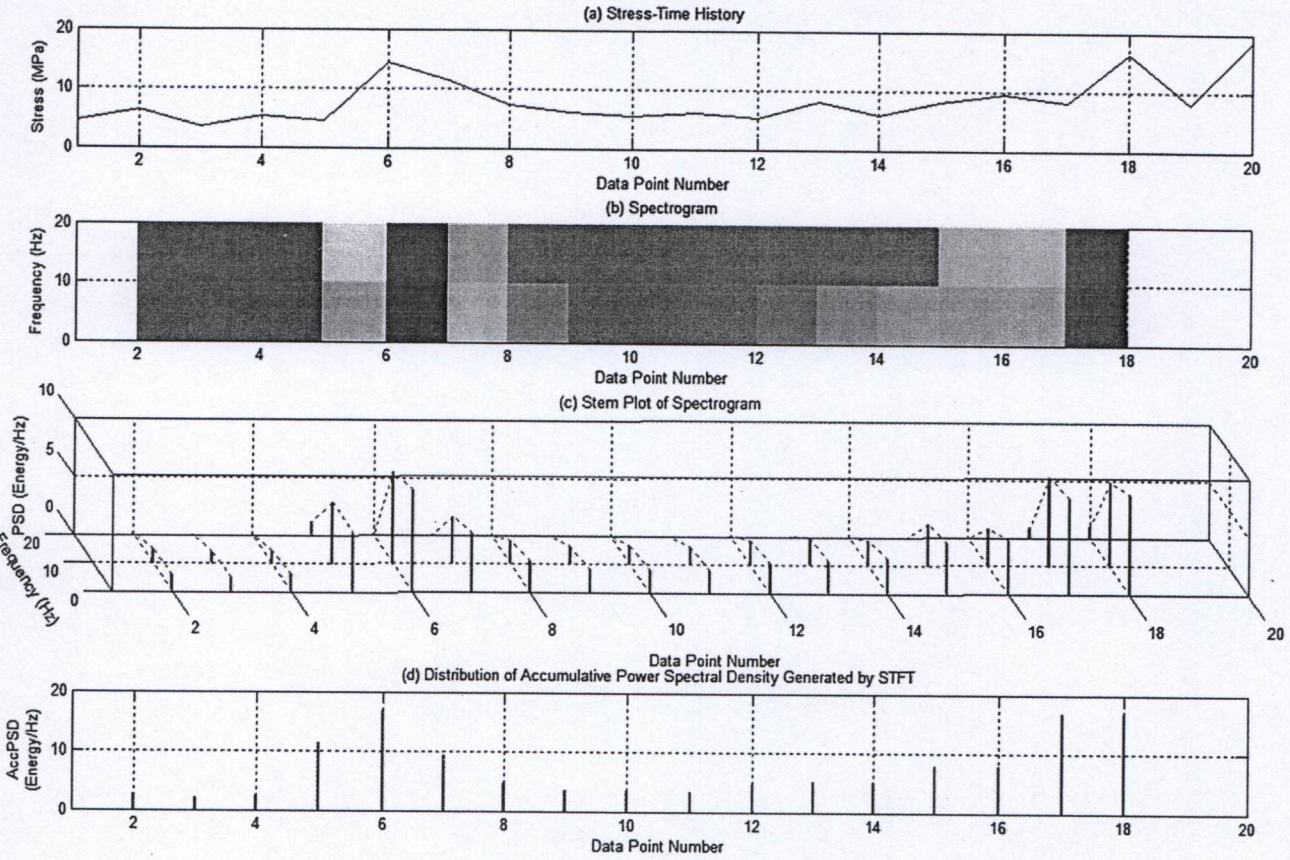

Fig. 2. Stress–time history, spectrogram, 3D-stem plot and AccPSD plot.

and 4 so there is no middle for these data points. Thus, Matlab locates AccPSD spike *1* at data point 2.

Based on a cutoff level represented by a dashed line in the second plot of Fig. 3, no extractions need to be done for windows 1–3 because the amplitudes of AccPSD spikes *1* to *3* are lower than the cutoff level. For window 4, the amplitude of AccPSD spike *4* is higher than the cutoff level so the data points 4, 5, 6 and 7 are extracted from the typical stress–time history and formed the damage segment 1. In the same manner, the amplitudes of AccPSD spikes *5* and *6* are higher than the cutoff level so data points 5, 6, 7, 8 and data points 6, 7, 8, 9 are extracted and formed the damage segments 2 and 3, respectively. By superposing the damage segments 1, 2 and 3, the damage part 1 is formed by data points 4, 5, 6, 7, 8 and 9. Similarly, the damage part 2 is formed by superposing damage segments 4, 5, 6 and 7. Eventually, damage parts 1 and 2 are concatenated to form the edited stress–time history as shown in the bottom plot of Fig. 3.

3. Theory

3.1. Fourier transform

Mathematically, Fourier discrete expansion, Eq. (2), is used to break down a complicated signal into three types of simple waves which are sine waves, cosine waves and a straight wave. Wave a_0 is a straight wave that indicates how far the entire complex periodic wave is displaced above or below zero. The periods of the sine and cosine waves are integral multiples of the period of $x(t)$. Amplitudes a_n and b_n show how much of each sine and cosine wave the complex periodic wave contains. Both sine and cosine waves have frequencies that are integral multiples of a fundamental frequency. The time it takes for a wave to oscillate once is called period T. The number of times a wave oscillates in 1 s is called frequency f. The relationship between the period and the frequency is given by $f = 1/T$. The angle rotated in 1 s (in radians per second) is called angular velocity. The relationship between the angular velocity and the frequency is given by $\omega = 2\pi f$.

$$x(t) = a_0 + \sum_{n=1}^{\infty} (a_n \cos n\omega t + b_n \sin n\omega t) \tag{2}$$

Complex number of representation of Fourier series in Eq. (2) is [21]

$$x(t) = \sum_{n=-\infty}^{\infty} C_n \exp(in\omega t) = \sum_{n=-\infty}^{\infty} C_n \exp(i2\pi f_n t) \tag{3}$$

where $i = \sqrt{-1}$ is the imaginary unit and C_n is the complex number representation of Fourier coefficients.

$$C_n = \frac{1}{T} \int_{t=0}^{t=T} x(t)\exp(-i2\pi f_n t)\mathrm{d}t \tag{4}$$

The relationship between the period and the fundamental frequency is $\Delta f = 1/T$. If the wave takes infinite time to advance through one period, then its frequency is extremely close to zero since the wave passes through only the tiniest function of its period in 1 s. When the fundamental frequency approaches zero, the interval between frequencies on the spectrum grows narrower and narrower as typically shown in Fig. 4. In other words, the longer the

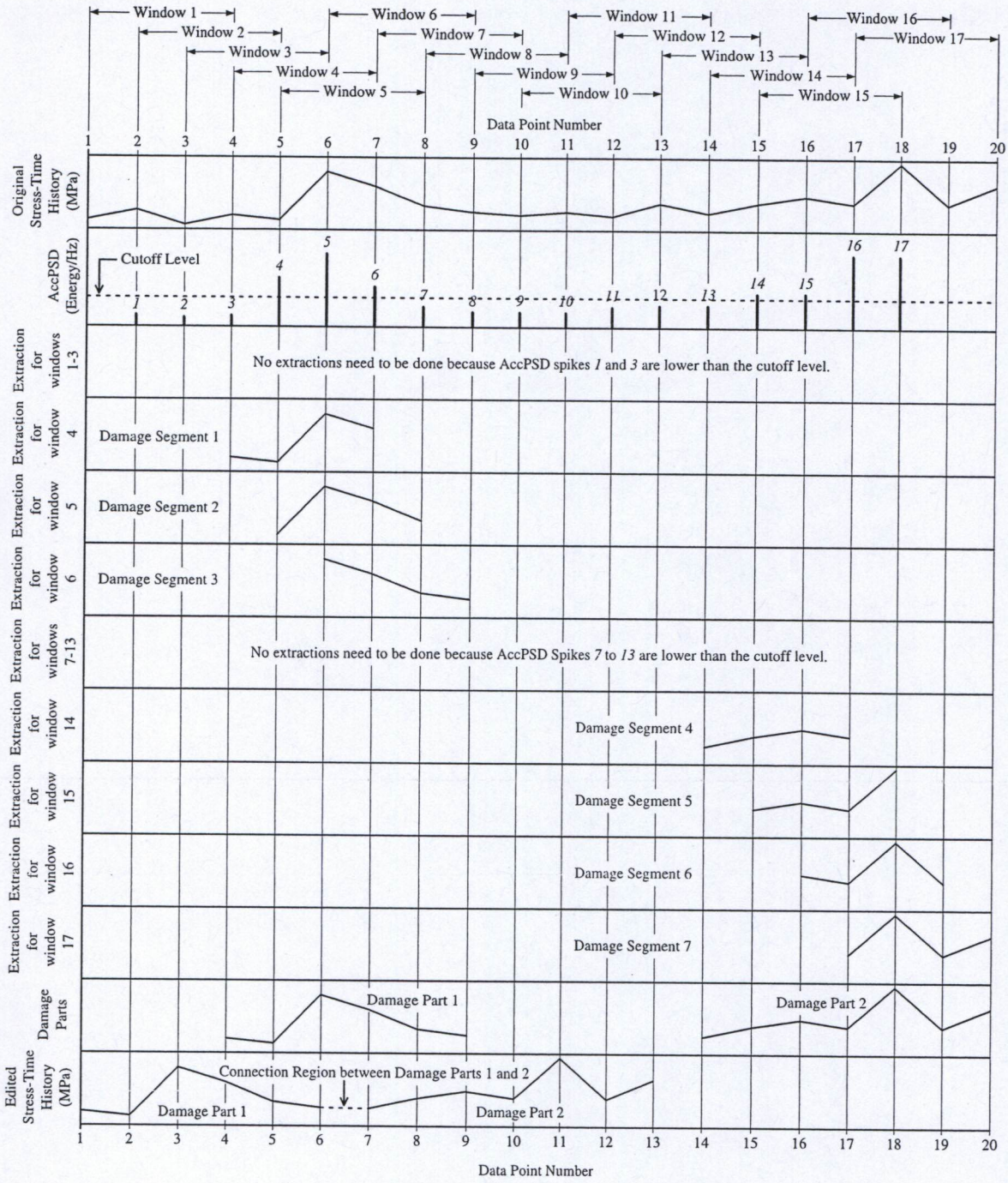

Fig. 3. Algorithm for extracting fatigue damage parts.

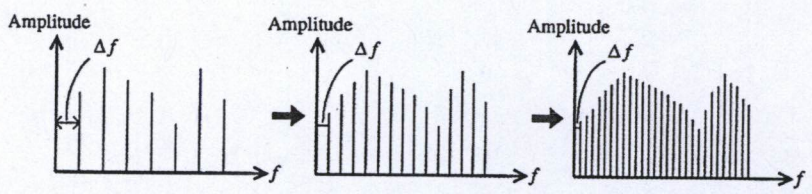

Fig. 4. Spectrum of a wave.

period is, the shorter the interval is between spectrum frequencies. Eventually, when the period reaches infinity, the spectrum becomes a continuum with no gap between frequencies. Thus, all frequencies become known when the period is infinity, even those that were not apparent through Fourier coefficients formula. Fourier transform of a signal $x(t)$ is

$$G(f_n) = \frac{1}{T}\int_{-\infty}^{+\infty} x(t)\exp(-i2\pi f_n t)dt \tag{5}$$

The frequency composition of a random function can be described in terms of the spectral density of mean square value [22]. Mean square value of a periodic time function is the sum of the mean square of the individual harmonic component.

$$\overline{x^2} = \sum_{n=1}^{\infty}\frac{1}{2}C_n C_n^* \tag{6}$$

Thus, $\overline{x^2}$ is made up of discrete contributions in each frequency interval or frequency band Δf.

First, one defines the contribution to the mean square in the frequency band as the *power spectrum* $G(f_n)$.

$$G(f_n) = \frac{1}{2}C_n C_n^* \tag{7}$$

Then, the mean square is

$$\overline{x^2} = \sum_{n=1}^{\infty} G(f_n) \tag{8}$$

Now, one defines the discrete *power spectral density* $S(f_n)$ as the power spectrum divided by the frequency band.

$$S(f_n) = \frac{G(f_n)}{\Delta f} = \frac{C_n C_n^*}{2\Delta f} \tag{9}$$

The mean square value can then be rewritten as

$$\overline{x^2} = \sum_{n=1}^{\infty} S(f_n)\Delta f \tag{10}$$

Power spectral density (PSD) is a normalised density plot describing the mean square amplitude of each sinusoidal wave with respect to its frequency. PSD shows the strength of the variations (energy) as a function of frequency. It shows at which frequencies, variations are strong and at which frequencies, variations are weak. The unit of PSD is energy per Hz (frequency width) and energy within a specific frequency range can be calculated by integrating PSD within that frequency range. Computation of PSD can be done by fast Fourier transform (FFT).

3.2. Short-time Fourier transform

Using the Fourier transform, the frequency components of an entire signal can be analysed but it is not possible to locate at what point in time that a frequency component occurs. This is not problematic when a stationary signal is analysed. However, Fourier analysis is not suitable for non-stationary signals. If there is a time localisation due to a particular feature in a signal such as impulse, this will only contribute to the overall mean valued frequency distribution and feature location on the time axis is lost [23]. To solve this deficiency, Dennis Gabor [24] adapted the Fourier transform to analyse only a small section of the signal at a time. This technique is called windowing the signal. Gabor's adaptation is called the short-time Fourier transform (STFT) which maps a signal into a two-dimensional function of time and frequency.

The STFT represents a sort of compromise between the time- and frequency-based views of a signal. It provides some information about both when and at what frequencies a signal event occurs [25]. The STFT compromises between time and frequency information. However, this information can only be obtained with limited precision determined by the window length, which is chosen so as to relate the signal in time without any distortions. The STFT assumes that if a time-varying signal is divided into several segments, each segment can be assumed stationary for analysis purposes. Then, Fourier transform is applied to each segment using Gaussian window function which is nonzero in the segment being analysed and it is set to zero outside the segment [26].

The STFT was developed from Fourier transform and it is mathematically defined as

$$\mathrm{STFT} = X(\tau,f) = \int_{-\infty}^{+\infty} x(t)w(t-\tau)\exp(-i2\pi f)dt \tag{11}$$

where $x(t)\exp(-i2\pi f)$ is the Fourier transform of the windowed signal, w is the window function and τ is the time position of the window [27]. The result of the transformation is a number of spectra localised in each windowed segment.

3.3. Fatigue damage versus accumulative power spectral density

This section mainly discusses the concept of applying AccPSD to identify fatigue damage events contained in the stress–time history. For the purpose of illustration, segment 52 (a red signal in Fig. 12(a), in web version), is intentionally selected because it clearly shows where the damage and non-damage parts are. To generate the plot of AccPSD versus data point number (time location), signal processing toolbox in Matlab [20] is used. STFT is taken to segment 52 in Fig. 5(a) and then a spectrogram is generated as shown in Fig. 5(b). The spectrogram shows how the PSD of STFT coefficients distribute in time–frequency domain. The plot of AccPSD of segment 52 shown in Fig. 5(c) is derived from the spectrogram by summing the PSD of all frequency bands at each time interval.

At this stage, the plot of AccPSD does not have the knowledge to identify where the fatigue damage events are located in segment 52. To teach the plot of AccPSD knowledge, the time locations that fatigue damage occurs must be known. In this article, fatigue damage at time locations is known from TCFD. This method is used by commercial software [18]. Based on TCFD, the authors use a plot of fatigue damage versus data point number in Fig. 6(b) to teach AccPSD knowledge. The red signals in Fig. 6(a) (in web version) are marked by TCFD. They are non-damage parts which must be removed from segment 52. The black signals in Fig. 6(a) are damage parts. They are concatenated to form an edited segment 52 shown in Fig. 6(c).

To observe the distribution patterns among the fatigue damage obtained from TCFD and AccPSD obtained from STFT, Figs. 5(c) and 6(a,b) are displayed on the same figure, i.e. Fig. 7. Considering Fig. 7(a), the fatigue damage contained in each group of the black signals is implied by the amplitude of fatigue damage spikes shown in Fig. 7(b). It is noticeable that each spike indicates both where and how much the fatigue damage occurs.

By observing the distribution patterns of spikes, it has been found that almost all the spikes of AccPSD in Fig. 7(c) are located at time intervals that the spikes of fatigue damage are located in Fig. 7(b), especially at the positions 1–41. When comparing the amplitude of damage spikes to the amplitude of AccPSD spikes at each time interval, it has been found that the amplitude of AccPSD spikes does

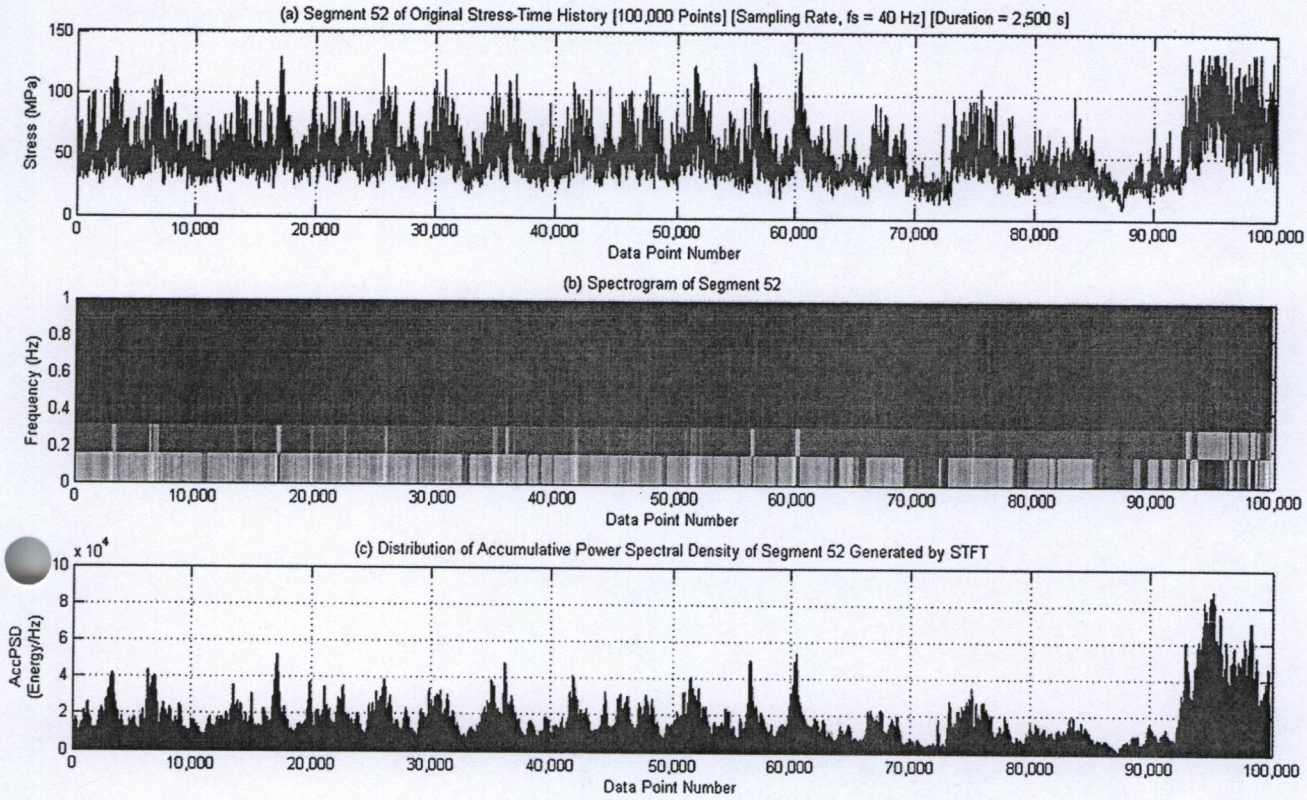

Fig. 5. Segment 52, spectrogram and AccPSD distribution generated by STFT.

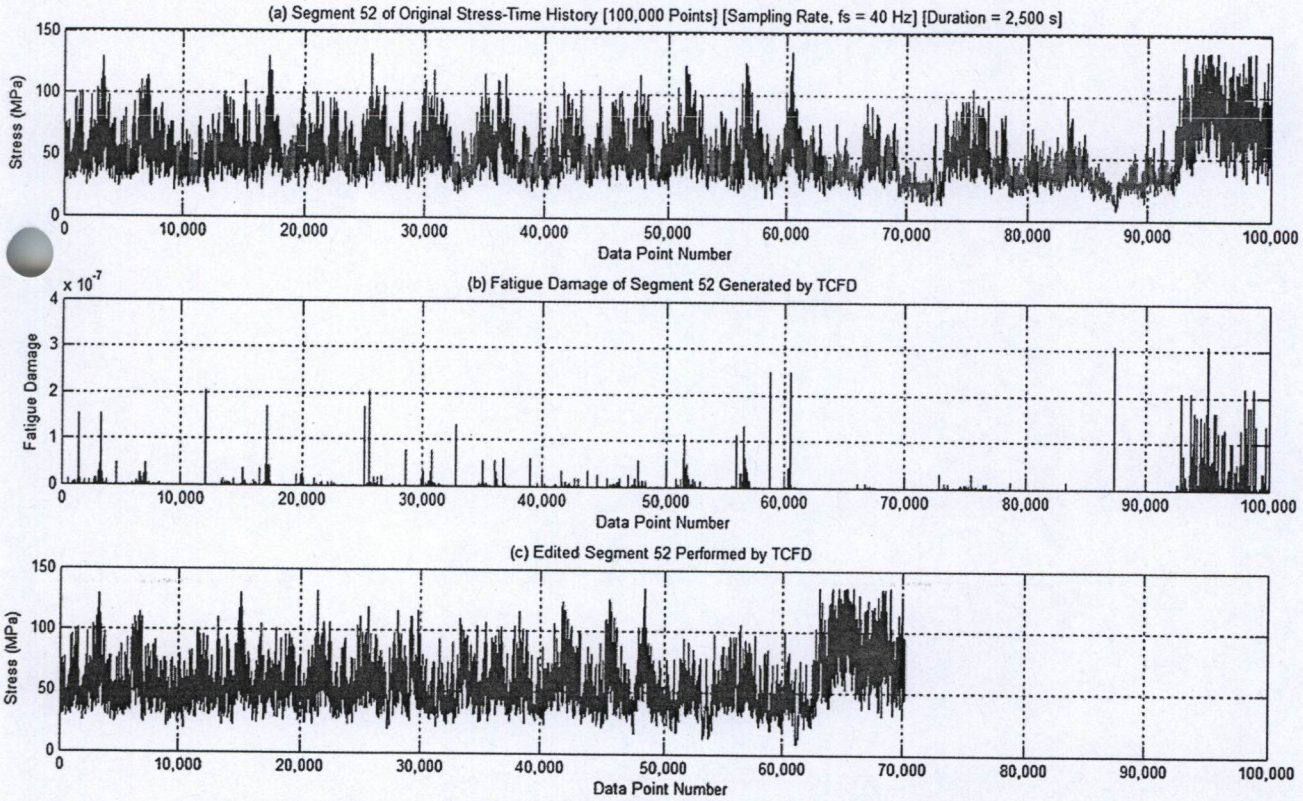

Fig. 6. Results of segment 52 generated by TCFD.

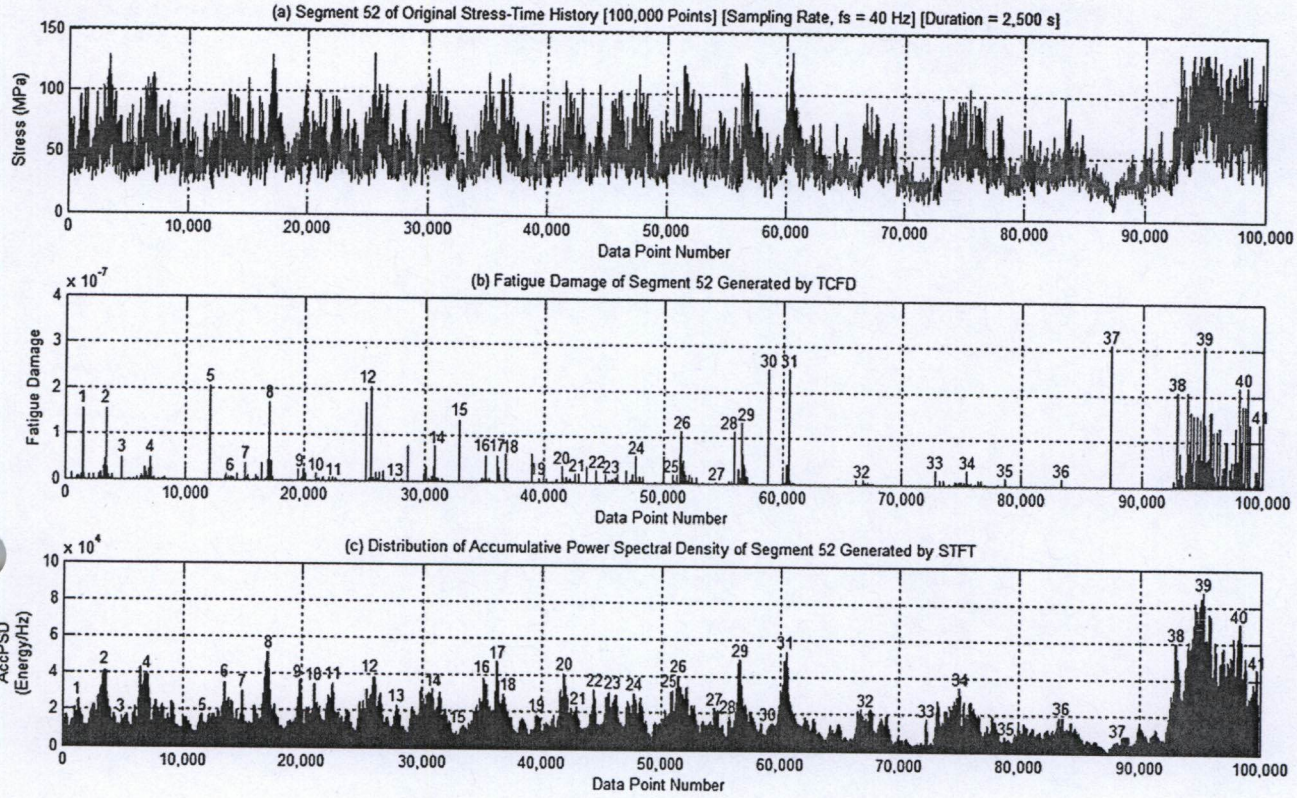

Fig. 7. Damage parts, non-damage parts, fatigue damage and AccPSD.

not tell us how much fatigue damage occurs. For example, there are same amplitudes of damage spikes located at points 1 and 2 but the amplitudes of AccPSD spike at point 1 are lower than that at point 2. The same situation occurs at points 30 and 31. Furthermore, it is outstanding that there is a high peak of damage spike at point 37 but the amplitude of AccPSD spike at the same point is very low. Fortunately, it is clearly seen that the locations of each spike of AccPSD tell us where the fatigue damage occurs.

Next idea is that in which spikes the plots of AccPSD should be used to identify the locations of fatigue damage. The authors try to hide the bottom parts of AccPSD plot by using white rectangles with different heights shown in Fig. 8(b–d). The upper edge of each rectangle is called cutoff level. With cutoff levels of 10,000 and 15,000 Energy/Hz, Fig. 8(b) and (c) removed peaks 15, 35 and 37. By increasing the cutoff level to 20,000 Energy/Hz as shown in Fig. 8(d), it has been found that the peaks 5, 15, 19, 28, 30, 33, 35, 36 and 37 are removed. In this manner, it is noticeable that the pattern of each group of peaks left in Fig. 8(d) resembles the pattern of fatigue damage in Fig. 8(a).

For the subject matter mentioned in this section, three issues based on observation can be summarised.

1. The amplitudes of AccPSD spikes do not indicate how much fatigue damage occurs.
2. The locations of AccPSD spikes, which are observed manually, are close to the locations of the fatigue damage that occurred.
3. The fatigue damage events in the stress–time history could be identified by an appropriate cutoff level.

The cutoff level is very important because it is used as a criterion in identifying and extracting fatigue damage parts from the original stress–time history. The signal segments which have levels of AccPSD equal to or higher than cutoff level will be identified as the damage parts and vice versa for the non-damage parts. By this criterion, the damage parts will be extracted from the original stress–time history and then they are concatenated to form an edited stress–time history. Ideally, the fatigue damage contained in the edited stress–time history should be the same as the original damage. If the cutoff level is too high, the minority of fatigue damage events will be detected; consequently, the length of the edited stress–time history is very short. Also, the retained fatigue damage will dramatically deviate from the original fatigue damage. On the other hand, if the cutoff level is too low, some non-damage parts may be identified as the damage parts; consequently, the length of the edited stress–time history may be slightly reduced whilst the retained fatigue damage may not be changed or a little bit from the original fatigue damage. To determine the appropriate cutoff level, the effect of cutoff level on fatigue damage retained in the edited stress–time history has been discussed in Section 4.

The observation done in this section implies that the plot of AccPSD gained from the spectrogram enables us to identify the fatigue damage events contained in the original stress–time history.

4. Window size effect on variation of fatigue damage per repetition

In the process, STFT is taken to the original stress–time history shown in Fig. 12(a) by using signal processing toolbox in Matlab [18]. The question is what window size (nfft) should be used in taking STFT. No procedure for choosing the best window size of STFT has been proposed yet. Comparative study is the only way to find an optimal window size of STFT. To answer this question, the window size effect on variation of fatigue damage per repetition needs to be studied before editing the stress–time history by STFT.

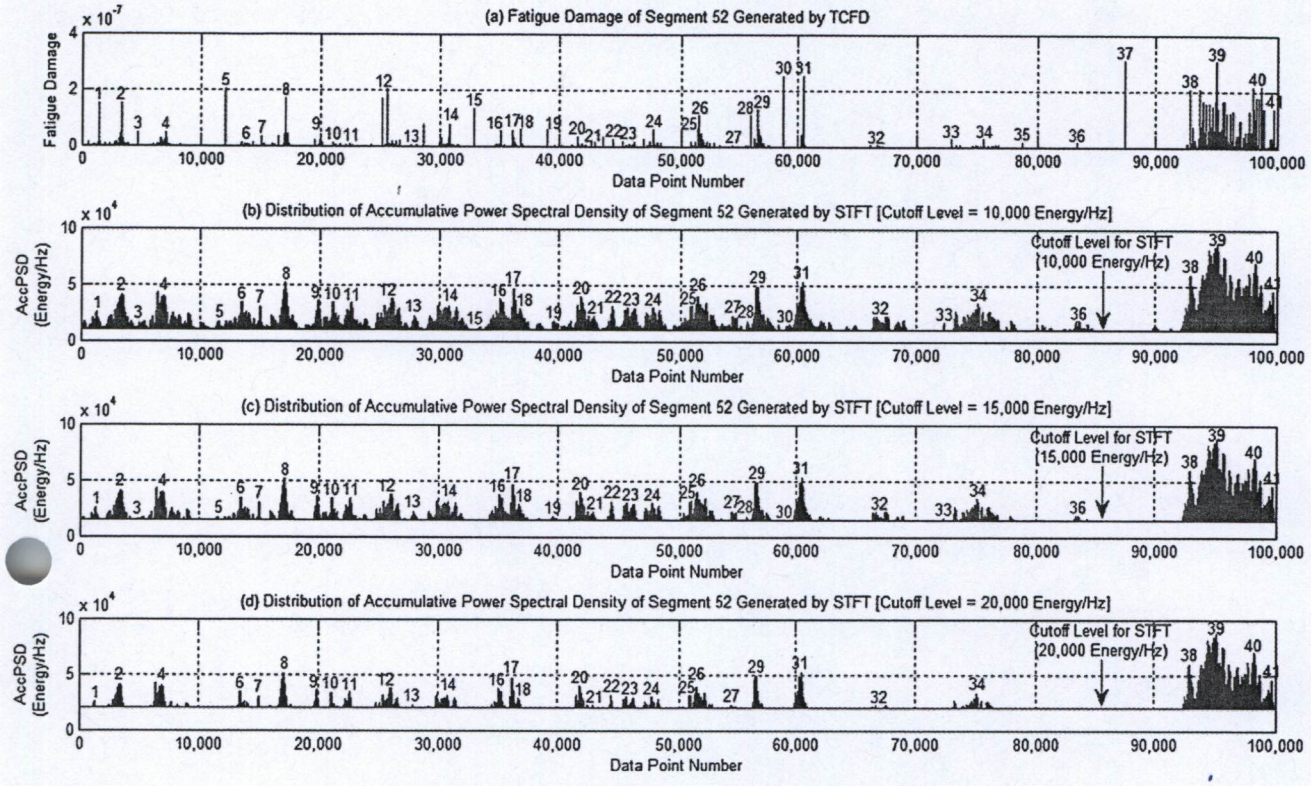

Fig. 8. Fatigue damage and AccPSDs generated by STFT with three different cutoff levels.

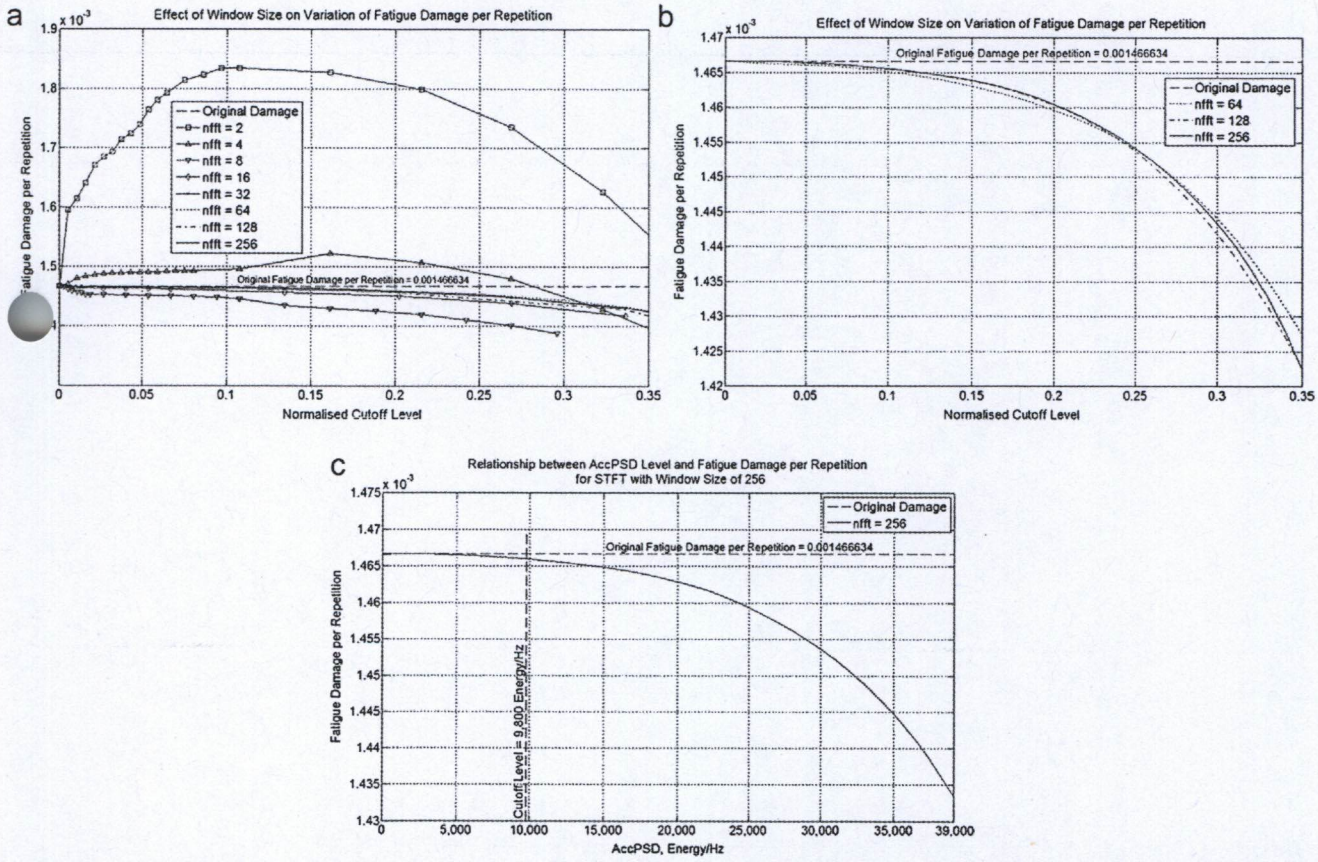

Fig. 9. Effect of window size on fatigue damage per repetition: (a) nfft 2 to 256; (b) nfft 64, 128 and 256; (c) nfft 256.

Table 1
Data from varying window size.

nfft	Cutoff level (Energy/Hz)	% reduction in length of the edited history	% error			
			Fatigue damage per repetition	Mean stress	rms	Kurtosis
2	5	2.11	−8.716	+0.28	+0.17	−1.28
4	110	13.48	−1.695	−9.01	−5.74	−5.49
8	200	11.56	+1.069	−7.34	−4.69	−6.96
16	500	13.78	+0.334	−8.97	−5.86	−13.45
32	1000	13.24	+0.176	−8.42	−5.54	−15.14
64	2000	13.04	+0.062	−8.19	−5.42	−16.56
128	4800	15.31	+0.042	−9.91	−6.63	−22.35
256	9800	15.38	+0.045	−9.92	−6.66	−23.45

Note: (+) and (−) signs of percent error mean less than and greater than, respectively.

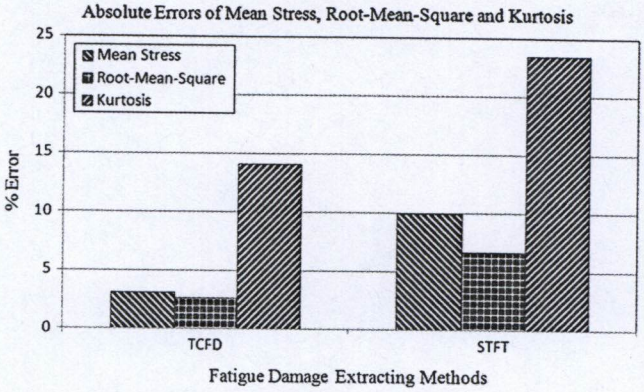

Fig. 10. Differences in signal statistical parameters.

The STFT is taken to the original stress–time history with window sizes of 2, 4, 8, 16, 32, 64, 128, and 256 points, respectively. For each window size, cutoff levels are varied and then the original stress–time history is edited. The fatigue damage per repetition of each edited stress–time history is evaluated. Consequently, the relationships between normalised cutoff level and fatigue damage per repetition for each window size can be established as shown in Fig. 9(a).

Since each window size of STFT taken to the same segment of the original stress–time history provides the different levels of AccPSD, all relationships cannot be compared directly. They must be normalised by their corresponding maximum levels existing in the original stress–time history. Fig. 9(a) shows the relationships between normalised cutoff level and fatigue damage per repetition for window sizes of 2, 4, 8, 16, 32, 64, 128 and 256 points. The dashed line represents the original level of fatigue damage per repetition. At this stage, the authors want to know which window size should be used in taking STFT. By means of three criteria, only one curve must be selected from this group. The first criterion is that the difference in fatigue damage per repetition must not be greater than ±10%. The second criterion is that the differences in mean stress, root-mean-square (rms) and kurtosis must not be greater than ±10% [28–30]. The third criterion is that the length of the edited stress–time history must be the shortest one compared to each other.

The curves in Fig. 9(a) could be separated into two groups. The first group shows that the fatigue damage increases beyond the original level and then decreases near the end of the range being considered. The curves in this group are for window sizes 2 and 4. They should not be taken into account because their differences of fatigue damage per repetition are very high compared to others (see Table 1). The second group shows that the fatigue damage decreases when the normalised cutoff level increases. Although all curves in this group show the desired behaviour, the curves for window sizes of 8, 16 and 32 can be removed from the group

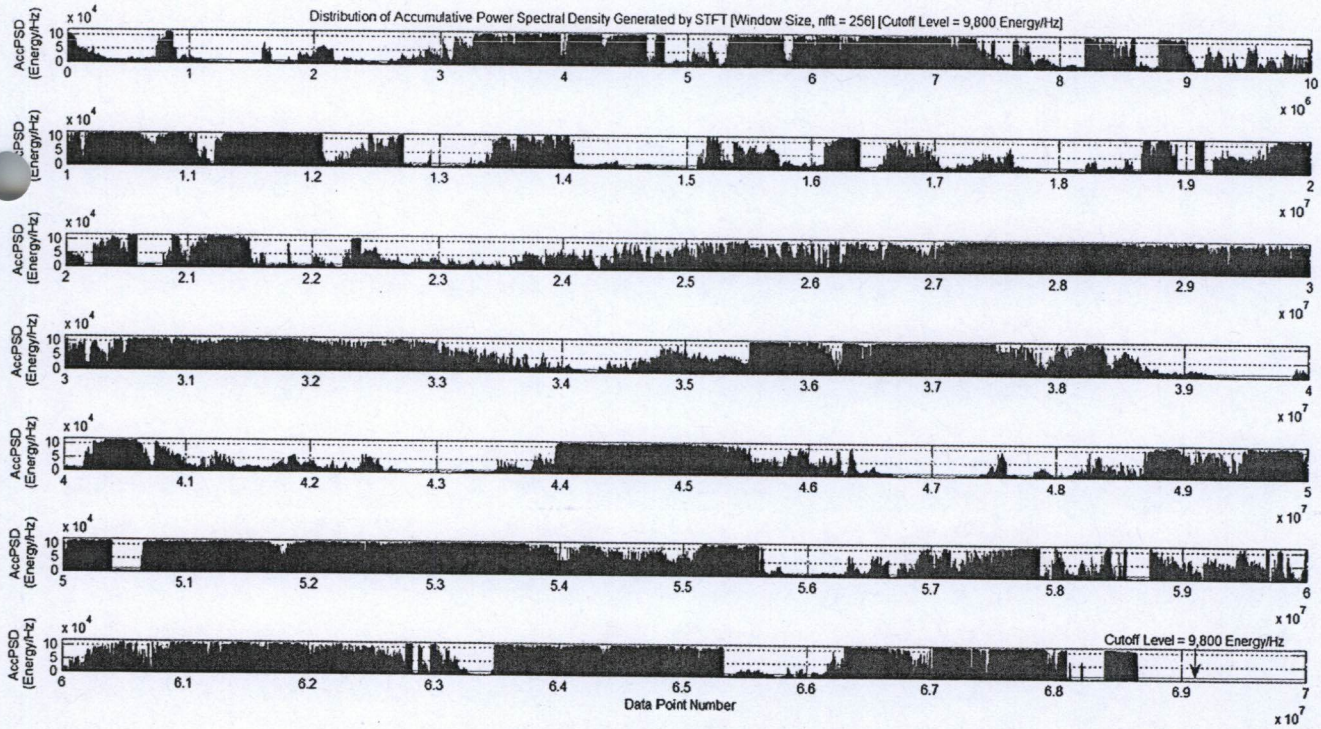

Fig. 11. A plot of AccPSD distribution generated by STFT.

because of the rapid change in damage values near the beginning of the range being considered. Thus, the curves for window sizes of 64, 128 and 256 are still candidates. Considering Fig. 9(b), all curves show that the fatigue damage slightly decreases at the beginning and rapidly drops when the value of normalised cutoff level is beyond 0.1. It is difficult to select one of them with the naked eye. To select the best curve, the data listed in Table 1 are considered. It is found that all window sizes satisfy all criteria except the error of kurtosis. The window sizes of 128 and 256 appear to not differ in results. But the shortest length of the edited stress history is the desired result, so the window size of 256 shown in Fig. 9(c) is selected as the representative in taking STFT.

To summarise, window size of 256 and cutoff level of 9800 Energy/Hz (see Table 1) provided the best result. The plot of AccPSD

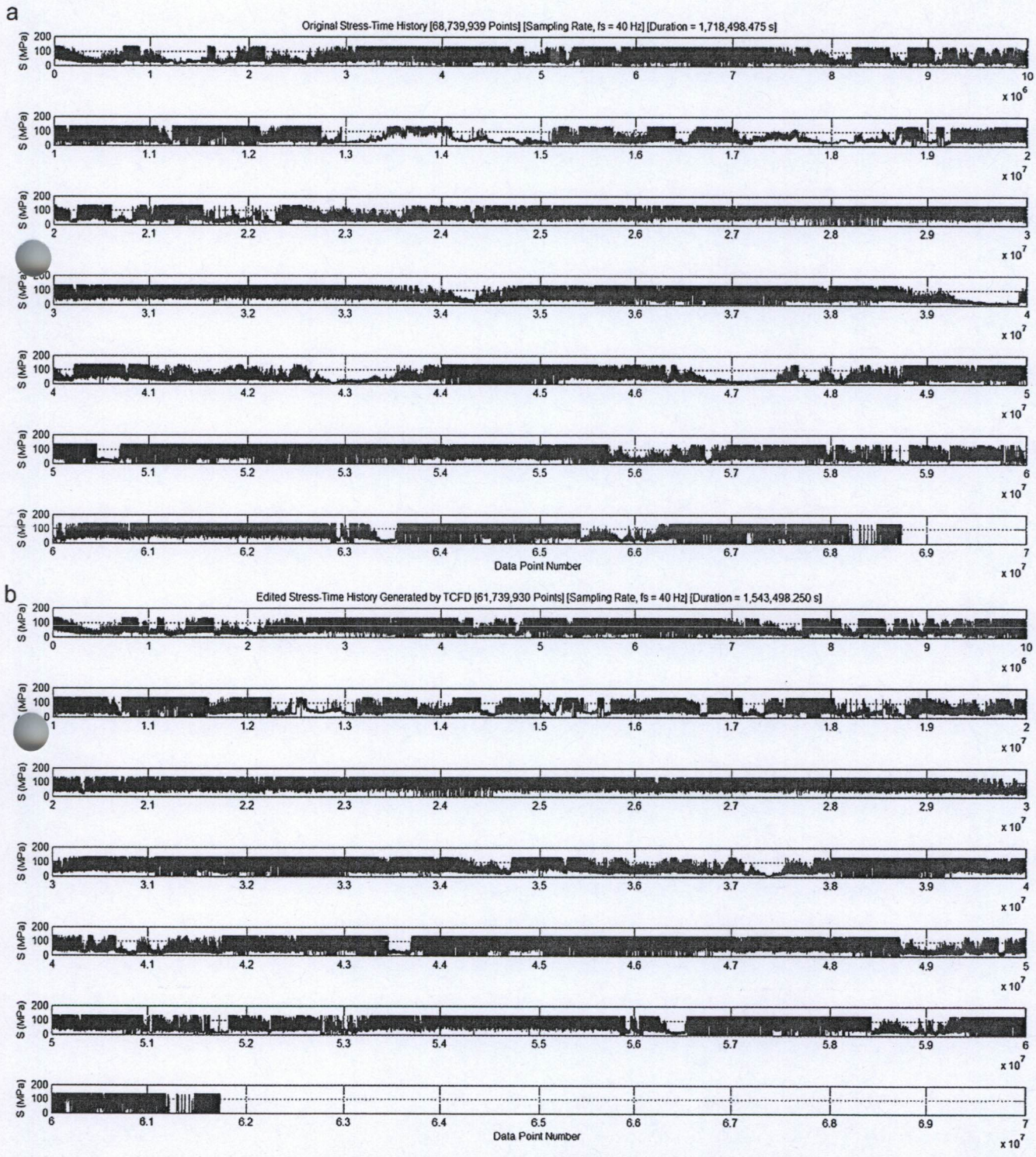

Fig. 12. Stress–time histories: (a) Original; generated by (b) TCFD; (c) STFT.

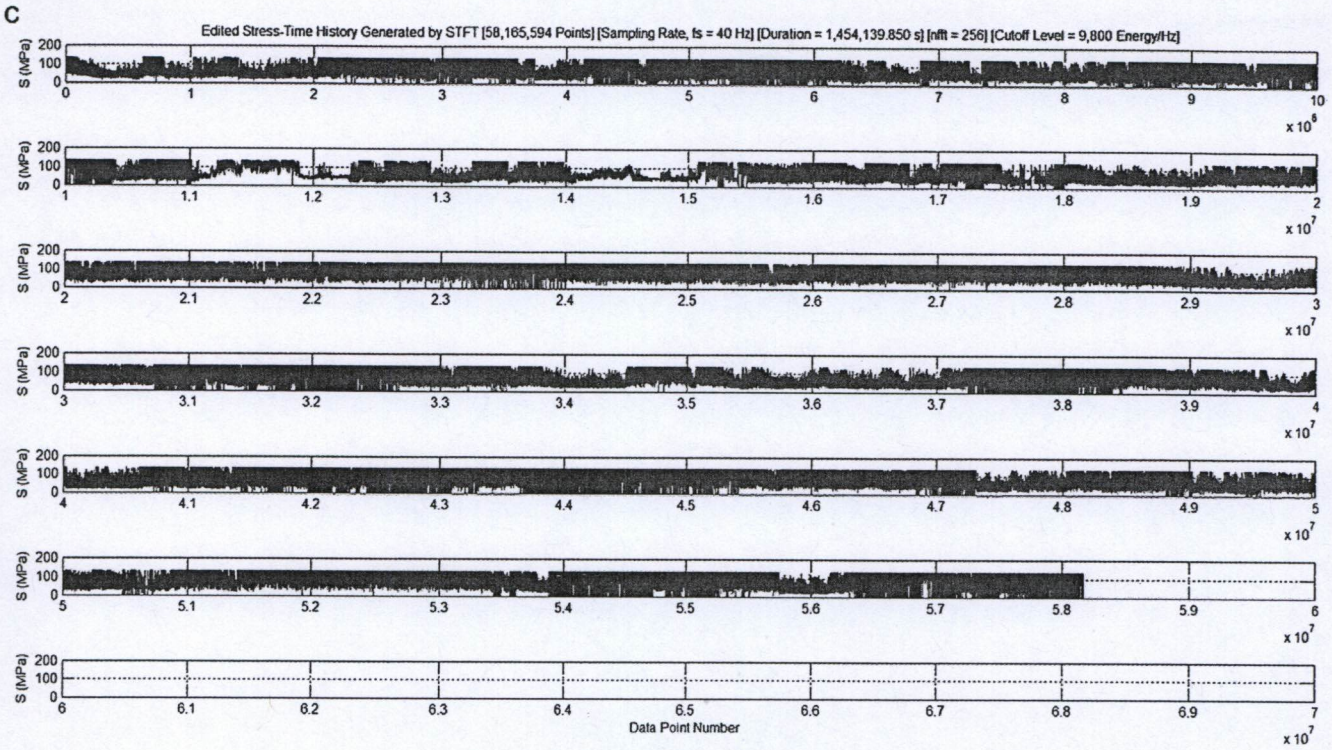

Fig. 12. (*continued*).

is shown in Fig. 11. The edited stress–time history has a reduction of 15.38% in length with respect to the original length. In other words, the length of the edited stress–time history is 84.62% of the original length. The difference in fatigue damage per repetition is +0.045% whilst the differences in mean stress and root-mean-square of the edited stress–time history are within ±10%, except for kurtosis (see Fig. 10).

5. Results and discussion

The original stress–time history in Fig. 12(a) is edited by TCFD and STFT. The first method is done in the time domain whilst the second method is done in the time–frequency domain. TCFD removes non-damage sections on the basis of time correlated fatigue damage windows of the input signal. The signal is divided into a number of time segments. Then, fatigue damage is calculated for each time-window. Windows having minimal damage are removed. The retained windows are assembled together to produce the edited stress–time history shown in Fig. 12(b). The edited stress–time history has a reduction of 10.18% in length with respect to the original length (see Table 2). In other words, the length of the edited stress–time history is 89.82% of the original length. The difference in fatigue damage per repetition is +0.076% whilst the differences in mean stress and root-mean-square of the edited stress–time history are within ±10%, except for kurtosis.

For STFT, the window size effect on variation of fatigue damage per repetition is studied. It has been found that a window size of 256 points provides the shortest length of the edited stress–time history compared to the lengths provided by the window sizes of 64 and 128 points. Also, the differences in mean stress and root-mean-square in Table 2 are within ±10%, except for kurtosis. Furthermore, the result in Table 2 indicates that STFT has a high potential in identifying the fatigue damage events because the difference in fatigue damage per repetition is very much less than ±1%. Based on a cutoff level of 9800 Energy/Hz represented by a dashed line in Fig. 11, the events having AccPSD level higher than or equal to the cutoff level are classified as damage parts. Eventually, each damage part is concatenated to form the edited stress–time history shown in Fig. 12(c). The edited stress–time history has a reduction of 15.38% in length with respect to the original length. In other words, the length of the edited stress–time history is 84.62% of the original length. The difference in fatigue damage per repetition is +0.045% whilst the differences in mean stress and root-mean-square of the edited stress–time history are within ±10%, except for kurtosis.

The effectiveness of TCFD and STFT in extracting fatigue damage parts has been studied. Fig. 10 shows that the differences in both mean stress and root-mean-square for each method are quite the same pattern and they are within ±10%, whilst their differences in kurtosis are beyond ±10%. It is noteworthy that the differences in mean stress, root-mean-square and kurtosis for TCFD are less than those for STFT. Furthermore, it is shown that ±10% error of kurtosis cannot be used as a criterion for the given stress–time history. However, Table 2 shows that both methods provide the difference in fatigue damage per repetition at less than ±1%. Thus, it is indicated that each method has high potential in identifying fatigue damage events, especially STFT. Having considered the length of

Table 2
Summary results.

Method	Cutoff level (Energy/Hz)	% reduction in length of history	% error			
			Fatigue damage per repetition	Mean stress	rms	Kurtosis
TCFD	–	10.18	+0.076	−3.04	−2.64	−14.05
STFT	9800	15.38	+0.045	−9.92	−6.66	−23.45

Note: (+) and (−) signs of percent error mean less than and greater than, respectively.

the edited stress–time histories, STFT provides 84.62% of the original length whilst TCFD provides 89.82%.

6. Conclusions

At present, the concept of using STFT in editing stress–time history of HAWT blades is not proposed by any researchers. The STFT can be used to edit stress–time history of HAWT blades. The edited stress–time history is generated from the combination of damage parts. The edited stress–time history should have equivalent global signal statistics and fatigue damage to the original stress–time history. Since STFT is defined here for the first time, experimental validation of the algorithm is important.

The edited stress–time histories obtained from each method retains the fatigue damage per repetition at almost the same level as the original damage. This indicates that TCFD and STFT can be used with high confidence. TCFD provided an edited stress–time history as 89.82% of the original length whilst STFT provides 84.62% of the same original length. Under the purpose of accelerated fatigue test, the capabilities of STFT and TCFD in extracting fatigue damage from the stress–time history of HAWT blades have been compared. It has been found that, STFT has two factors that can have an effect on the fatigue damage extraction. They are window size and cutoff level. Furthermore, it has been found that STFT has two advantages. Firstly, STFT provided a shorter length of the edited stress–time history than TCFD. Secondly, STFT can improve the accuracy of the fatigue damage retained in the edited stress–time history. Although the differences in mean stress, root-mean-square, and kurtosis provided by TCFD are lower than those provided by STFT, they are only used to maintain the signal statistical parameters, so as not to change beyond ±10%.

To conclude, the edited stress–time history can be normally used in the durability laboratory scale fatigue test to accelerate fatigue testing. Finally, STFT is suggested as the alternative technique in fatigue durability study, especially for the field of wind turbine engineering.

Acknowledgements

The authors would like to thank the Royal Thai Government Scholarship for financial support.

References

[1] Sutherland HJ. On the fatigue analysis of wind turbines. Sandia National Laboratories; 1999. [SAND99–0089].
[2] British Standards Institution. Wind turbine generator systems – part 23: full-scaled structural testing of rotor blades. DD IEC TS 61400-23:2002; 2002.
[3] Marin JC, Barroso A, Paris F, Canas J. Study of fatigue damage in wind turbine blades. Eng Fail Anal 2009;16:656–68. http://dx.doi.org/10.1016/j.engfailanal.2008.02.005.
[4] British Standards Institution. Eurocode 3: design of steel structures – part 1–9: fatigue. BS EN 1993-1-9:2005; 2005.
[5] British Standards Institution. Wind turbines – part 1: design requirements. BS EN 61400-1:2005; 2005.
[6] Frost NE, Marsh KJ, Pook LP. Metal fatigue. Oxford University Press; 1974.
[7] Schluter LL, Sutherland HJ. User's guide for life2's rainflow counting algorithm. Sandia National Laboratories; 1991. p. 1–37. [SAND90-2259].
[8] Buhl ML Jr. NWTC Design Codes (MCrunch by Marshall Buhl) (alpha v1.00.00y-mlb, 8.4 MB, 21st May 2010, file: CompFatigue.m, 60 kB) [Computer Program] Matlab, Command line: 981–1089. Last modified 25th October 2010, Distributor: National Wind Technology Center; 2010.
[9] Fuchs HO, Nelson DV, Burke MA, Toomay TL. Shortcuts in cumulative damage analysis. In: Wetzel RM, editor. Fatigue under complex loading: analyses and experiments, vol. 6. The Society of Automotive Engineers Adv Eng; 1977. p. 145–62.
[10] Nelson DV, Fuchs HO. Predictions of cumulative fatigue damage using condensed load histories. In: Wetzel RM, editor. Fatigue under complex loading: analyses and experiments, vol. 6. The Society of Automotive Engineers Adv Eng; 1977. p. 163–87.
[11] Stephens RI, Fatemi A, Stephens RR, Fuchs HO. Metal fatigue in engineering. 2nd ed. New York: John Wiley & Sons; 2001.
[12] Ong CH, Tsai SW. The use of carbon fibers in wind turbine blade design: a SERI-8 blade example. Sandia National Laboratories; 2000. p. 1–69. [Report No. SAND2000-0478].
[13] Mandell JF, Samborsky DD. DOE/MSU composite material fatigue database March 31, 2010 version 19.0. Sandia National Laboratories; 2010.
[14] Sutherland HJ, Mandell JF. Effect of mean stress on the damage of wind turbine blades. J Sol Energy Eng 2004;126:1041–9. http://dx.doi.org/10.1115/1.1785160.
[15] Pratumnopharat P, Leung PS. Validation of various windmill brake state models used by blade element momentum calculation. Renew Energy 2011;36:3222–7. http://dx.doi.org/10.1016/j.renene.2011.03.027.
[16] Camp TR, Morris MJ, van Rooij R, van der Tempel J, Zaaijer M, Henderson A, et al. Design methods for offshore wind turbines at exposed sites. Garrad Hassan and Partners, Ltd; 2003. p. 1–65. [Report No. 2317/BR/22D].
[17] Pratumnopharat P, Leung PS, Court RS. Application of Morlet wavelet in the stress–time history editing of horizontal axis wind turbine blades. In: 2nd international symposium on environment-friendly energies and applications (EFEA 2012). Newcastle upon Tyne, United Kingdom 25–27 June 2012; 2012. p. 396–401. http://dx.doi.org/10.1109/EFEA.2012.6294048.
[18] ANSYS 13.0 nCode DesignLife, DesignLife theory guide, HBM-nCode; 2012. p. 1–210.
[19] Miner MA. Cumulative damage in fatigue. J Appl Mech 1945;12:A159–64.
[20] Matlab user's guide, signal processing toolbox for use with Matlab, user's guide version 4.2. The Mathworks Inc.; 1999.
[21] Gleason A. Who is Fourier? A mathematical adventure. Boston: Language Research Foundation; 2006.
[22] Thomas WT, Dahleh MD. Theory of vibration with applications. 5th ed. New Jersey: Prentice Hall, Inc.; 1998.
[23] Newland NE. An introduction to random vibrations, spectral and wavelet analysis. 3rd ed. Mineola, New York: Dover Publications Inc.; 1993.
[24] Gabor D. Theory of communication; 1944.
[25] Misiti M, Misiti Y, Oppenheim G, Poggi JM. Wavelet toolbox for use with Matlab, user's guide version 1; 1997.
[26] Park TH. Introduction to digital signal processing – computer musically speaking. New Jersey: World Scientific; 2010.
[27] Chui CK. An introduction to wavelets. San Diego: Academic Press; 1992.
[28] Abdullah S, Nizwan CKE, Nuawi MZ. A study of fatigue data editing using the short-time Fourier transform (STFT)'. Am J Appl Sci 2009;6:565–75.
[29] Abdullah S, Putra TE, Nuawi MZ, Nopiah ZM, Arifin A, Abdullah L. Time-frequency localization analysis for extracting fatigue damaging events. In: ISPRA'10 proceedings of the 9th WSEAS international conference on signal processing, robotics and automation; 2010. p. 31–5.
[30] Nopiah ZM, Abdullah S, Baharin MN, Putra TE, Sahadan SN, Willis KO. Comparative study on data editing techniques for fatigue time series signals. Adv Mater Res 2011;146–147:1681–4. http://dx.doi.org/10.4028/www.scientific.net./AMR.146-147.1681.

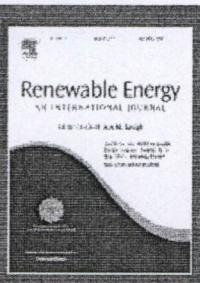

Renewable Energy

An International Journal

The Official Journal of WREN - The World Renewable Energy Network

The journal seeks to promote and disseminate knowledge of the various topics and technologies of **renewable energy** and is therefore aimed at assisting researchers, economists, manufacturers, world agencies...

View full aims and scope

Editor-in-Chief: A.A.M. Sayigh
View full editorial board

Guide for Authors
Submit Your Paper
Track Your Paper
Order Journal
View Articles

Impact Factor: 2.989

5-Year Impact Factor: 3.456

Imprint: ELSEVIER

ISSN: 0960-1481

Most Downloaded Articles

ScienceDirect

1. Barriers to renewable energy penetration; a framework for analysis
J.P Painuly

2. Bioethanol production from agricultural wastes: An overview
Nibedita Sarkar | Sumanta Kumar Ghosh | ...

3. Dynamic life cycle assessment (LCA) of renewable energy technologies
Martin Pehnt

VIEW ALL

Recent Articles

ScienceDirect

Hydrogen production from aqueous-phase reforming of sorghum biomass: An application of the response surface methodology
Bahar Meryemoğlu | Arif Hasanoğlu | ...

Carbon supported Ag nanoparticles with different particle size as cathode catalysts for anion exchange membrane direct glycerol fuel cells
Zhichao Wang | Le Xin | ...

A comprehensive study of dense-array

Conferences

Energy Systems Conference

VIEW ALL

Special Issues

World Renewable Energy Congress - Sweden, 8-13 May, 2011, Linkoping, Sweden
Volume 61 (2014)
ORDER NOW

The International Conference on Renewable Energy: Generation and Applications
Volume 56 (2013)
ORDER NOW

AFORE 2011(Asia-Pacific Forum of Renewable Energy 2011)
Volume 54 (2013)
ORDER NOW

VIEW ALL

Most Cited Articles

Scopus

Biodiesel production from oleaginous microorganisms
Meng, X. | Yang, J. | ...

Cellulase production using biomass feed stock and its application in lignocellulose saccharification for bio-ethanol production
Sukumaran, R.K. | Singhania, R.R. | ...

concentrator photovoltaic system using non-imaging planar concentrator
Fei-Lu Siaw | Kok-Keong Chong | ...

VIEW ALL

Determination of the density and the viscosities of biodiesel-diesel fuel blends
Alptekin, E. | Canakci, M.

VIEW ALL

Readers
View Articles
Volume/ Issue Alert

Authors
Author Information Pack
Submit Your Paper
Track Your Paper
Webshop

Librarians
Ordering Information and Dispatch Dates
Abstracting/ Indexing

Editors
Publishing Ethics Resource Kit
EES Support

Reviewers
Reviewer Guidelines
Log in as Reviewer

Advertisers/ Sponsors
Advertisers Media Information

Societies

Industries Advertising Careers Feedback Site Map Elsevier Websites A Reed Elsevier Company